Journal of Renewable Materials

Tech Science Press

DOI: 10.32604/jrm.2021.013884

ARTICLE

Preparation and Electrorheological Response of PAL/TiO_2/PANI Nanorods

Ling Wang[1,2], Chenchen Huang[1], Ping Zhang[3], Fenghua Liu[1,*], Ting Zou[1], Zhixiang Li[1], Jianfei Zhang[1] and Gaojie Xu[1]

[1]Ningbo Institute of Materials Technology and Engineering, Chinese Academy of Science, Ningbo, 315201, China

[2]Faculty of Materials Metallurgy and Chemistry, Jiangxi University of Science and Technology, Ganzhou, 341000, China

[3]Xuyi County Attapulgite Application Technology R&D and Achievement Transformation Center, Xuyi, 211700, China

[*]Corresponding Author: Fenghua Liu. Email: lfh@nimte.ac.cn

Received: 25 August 2020 Accepted: 03 November 2020

ABSTRACT

Using palygorskite (PAL) as template, the PAL/TiO_2/PANI nano-rods were synthesized by heterogeneous precipitation and in-situ polymerization. The synthesized PAL/TiO_2/PANI nanorods were used as a novel electrorheological (ER) fluid by mixing with silicone oil, which showed excellent ER effect. The yield stress of the PAL/TiO_2/PANI based ER fluid (15 vol%) reached 8.8 kPa under 4 kV mm^{-1} electric field. The dynamic shear stress of the PAL/TiO_2/PANI based ER fluid could maintain a stable level in the shear rate range of 0.1–100 s^{-1}. Furthermore, the PAL/TiO_2/PANI ER fluid exhibited excellent suspension stability.

KEYWORDS

Electrorheological; palygorkite; titanium oxide; polyaniline; nanorod

1 Introduction

Electrorheological (ER) fluid is a kind of intelligent material whose rheological properties can be readily controlled using an external electric field, which is formed by dispersing polarizable particles in insulating liquid [1,2]. Under the action of external electric field, the dispersed polarizable particles will attract each other to form fibrous structure, which leads to the significant increase of viscosity, yield stress and shear modulus of the suspension [3,4]. These changes are fast and reversible with the transformation of external electric field. Therefore, ER fluid has a wide range of application prospects in many fields, especially in automotive, aerospace and medical industries [5,6].

The performance of ER fluids is closely related to the polarization ability of dispersed particles, and the shape of dispersed particles is an important factor [7]. One dimensional nanomaterials, such as nanowires and nanotubes, are attractive new functional materials. The unique structural characteristics of one-dimensional nanomaterials are that one direction is nano and the other is micron, which not only makes one-dimensional nanomaterials show many novel properties, but also provides a coupling bridge between nano system and micro system [8,9]. Titanium oxide (TiO_2) and polyaniline (PANI) are considered to be the most promising two kinds of electrorheological materials [10–15] due to the high dielectric constant of TiO_2 and the adjustable conductivity of PANI. However, the one dimensional nano structure of TiO_2 and

PANI, especially the one-dimensional composite nano structure of TiO_2/PANI, is very difficult to synthesize, and the cost of preparation is very high.

In this paper, a novel one-dimensional PAL/TiO_2/PANI nanocomposite was prepared by heterogeneous precipitation of titanium oxide [16] and in-situ polymerization of Aniline [17], using the natural palygorkite (PAL) rods with high aspect ratio and large surface area as the heterogeneous nucleation center. The physical properties and ER characteristics of the obtained samples were investigated by SEM, TEM, XRD, IR, LCR Tester and rheometer. The results showed that the PAL/TiO_2/PANI particles were one-dimensional nano-structure and the phases of coating TiO_2 and PANI shells were amorphous. Compared with pure TiO_2 or PANI ER fluid, the polarization ability, electrorheological activity and suspension stability of PAL/TiO_2/PANI ER fluid were significantly improved.

2 Materials and Methods

2.1 Raw Materials

Ethanol(AR), ammonium hydroxide solution (25%~28%, AR), tetrabutyl titanate (TBOT, > 98%), aniline(An, AR), 38% hydrochloric acid (AR) and ammonium persulphate(APS, AR) were purchased from Sinopharm Chemical Reagent Company, Shanghai, China. Palygorkite was provided by Oil-better Limited Company, Xuyi, China.

2.2 Synthetize of PAL/TiO_2 Nanoparticles

The PAL/TiO_2 nanoparticles were prepared via the heterogeneous precipitation method [18]. 1.5 g PAL powder was dispersed in 400 ml absolute ethanol, placed in ultrasonic cell crusher for 30 min, and mixed with concentrated ammonia (2.30 ml, 28 wt%) to obtain PAL suspension. Then, 5 ml TBOT was added to the PAL suspension, and the reaction was allowed to proceed for 24 h under continuous mechanical stirring. After the reaction, the obtained milky white suspension was centrifuged, and the separated product was washed with ethanol for three times. Finally, the obtained white powder was dried in vacuum at 90°C for 20 h.

2.3 Synthetize of PAL/TiO_2/PANI Composites

The PAL/TiO_2/PANI composites were prepared by in-situ polymerization using the PAL/TiO_2 as carrier. 1.0 ml aniline monomer and 1 g PAL/TiO_2 were dispersed in 100 ml 0.1 mol/L HCl solution in a three-necked bottle. The mixtures were stirred with mechanical stirrers in ice water baths for 1 h to get a uniform suspension. Afterward, 100 ml pre-cooled 0.1 mol/L HCl solution containing 2.0 g APS was added by a peristaltic pump, and the reaction was allowed to proceed for 24 h under continuous mechanical stirring. After the reaction, the obtained blackish green suspension was centrifuged, and the separated product was washed with 50 wt% alcohol aqueous solution for three times. Finally, the obtained blackish green powder was dried in vacuum at 90°C for 20 h.

2.4 Synthetize of Pure TiO_2 and PANI

The pure TiO_2 was prepared by the way of the above ***2.2*** without the addition of PAL and the PANI was prepared by the way of the above ***2.3*** without the addition of PAL/TiO_2.

2.5 Preparation of ER Suspensions

Firstly, the insulating liquid dimethyl silicone oil was dried in vacuum at 110°C for 2 h, then the appropriate amount of powder material was added into the dimethyl silicone oil, and the ER suspensions with different solid contents were obtained by grinding for about 20 min. The density of dimethyl silicone oil is 0.940 g/cm^3 and the dielectric constant is 2.5.

2.6 Characterization

The microstructure and particle size of the samples were analyzed by SEM (Hitachi S4800) and TEM (FEI Tecnai G2 F20). The X-ray diffraction patterns of the particles were measured on a Rigaku D/Max-A diffractometer with CuKα radiation. The Infrared spectrum of samples was analyzed by Perkin Elmer system 2000 spectrophotometer. The dielectric properties of ER fluids in the frequency range of 50–10^5 Hz were determined by LCR tester (HIOKI 3532). The electrorheology of the ER fluids at different DC electric field was determined by a circular plate rheometer (Haake RS6000).

3 Results and Discussion

3.1 Material Characteristics

The morphologies and microstructure of the samples were characterized by SEM and TEM analysis as shown in Figs. 1 and 2. It can be seen from Figs. 1a and 2a that the pure PAL was a rodlike fiber with a length up to several micrometers and a width of 30∼50 nm. After introducing titanium oxide via the heterogeneous precipitation coating method, it was obvious that the surface of nanorods became coarse, and titanium oxide nanoparticles with a diameter of several nanometers were uniformly distributed on the surface of PAL nanorods (Figs. 1b and 2b). The SEM and TEM images of the PAL/TiO_2/PANI particles prepared by in-situ polymerization using the PAL/TiO_2 as carrier are shown in Figs. 1c and 2c. The results indicated that the PAL/TiO_2 particles had been successfully coated by PANI layers via the in-situ polymerization process and the thickness of the shell was about 20 nm.

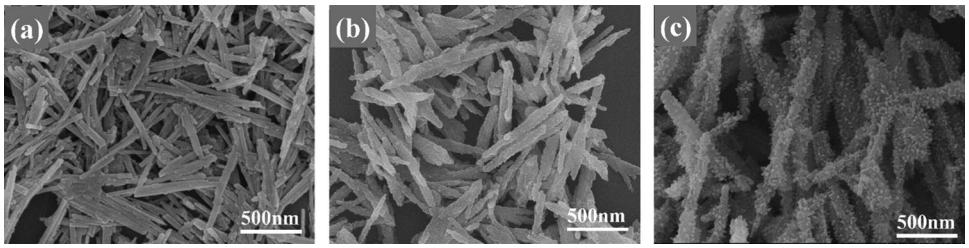

Figure 1: The SEM images of the PAL (a), PAL/TiO_2 (b), PANI and PAL/TiO_2/PANI (c)

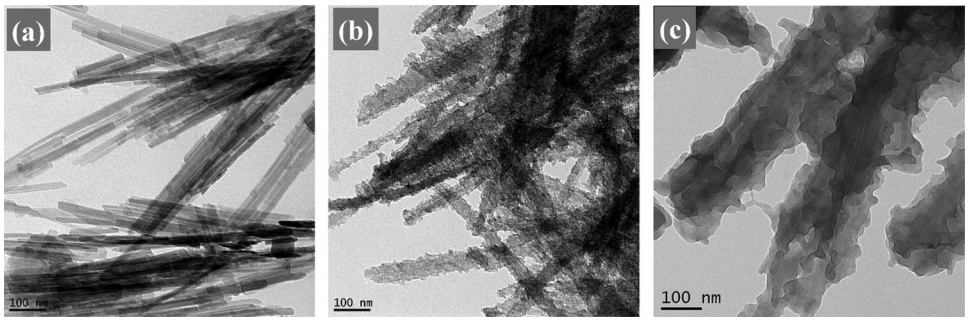

Figure 2: The TEM images of the PAL (a), PAL/TiO_2 (b) and PAL/TiO_2/PANI (c)

The X-ray diffraction patterns of the PAL, PAL/TiO_2 and PAL/TiO_2/PANI nanoparticles are shown in Fig. 3. The peak positions at 2θ values of 8.4, 13.9, 16.5, 19.8, 27.5, and 34.9 were correspondence to the characteristic diffraction peaks of PAL [19,20]. By comparing the XRD patterns of the PAL, PAL/TiO_2 and PAL/TiO_2/PANI, it is found that the three samples all have the diffraction characteristic peaks of PAL, and the phase of coated TiO_2 and PANI shell is amorphous. In addition, the diffraction characteristic peaks of PAL decreases gradually with the increase of shell thickness.

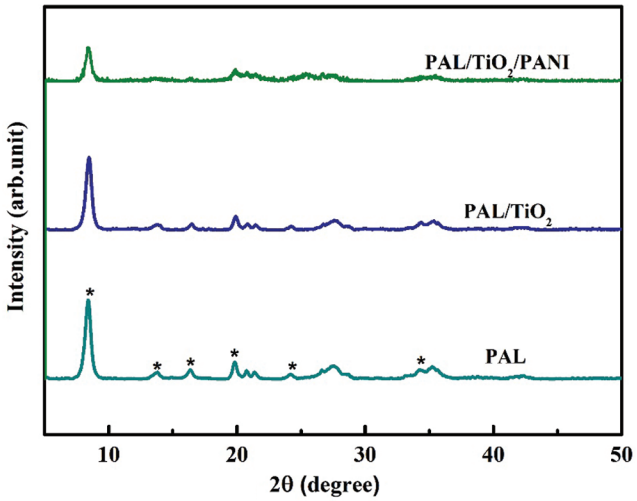

Figure 3: The X-ray diffraction patterns of the PAL, PAL/TiO_2 and PAL/TiO_2/PANI

The FT-IR spectra of the TiO_2, PANI and PAL/TiO_2/PANI are shown in Fig. 4. For the granular TiO_2, the broadband around 3400 cm^{-1} and the peak at 1630 cm^{-1} were associated with the vibrations of –OH, and the absorption band of 500–800 cm^{-1} was attributed to the stretching vibrations of Ti-O [12]. For the pure PANI, the bands at 1563 cm^{-1} and 1482 cm^{-1} were due to the stretching vibrations of quinonoid and benzenoid rings respectively, the bands at 1296 cm^{-1} and 1241 cm^{-1} were due to the C-N stretching mode for benzenoid ring and C=N stretching vibrations, while the bands at 1109 m^{-1} was assigned to a plane bending vibration of C-H [15]. For the PAL/TiO_2/PANI nanoparticles, the wavenumbers of 1040 cm^{-1} and 985 cm^{-1} could be attributed to the stretching vibrations of Si-O [21,22]. And all the characteristic peaks of titanium oxide and polyaniline can be found in the FT-IR spectra of the PAL/TiO_2/PANI. This indicates that TiO_2 and PANI are loaded on the surface of PAL by heterogeneous precipitation coating and in-situ polymerization.

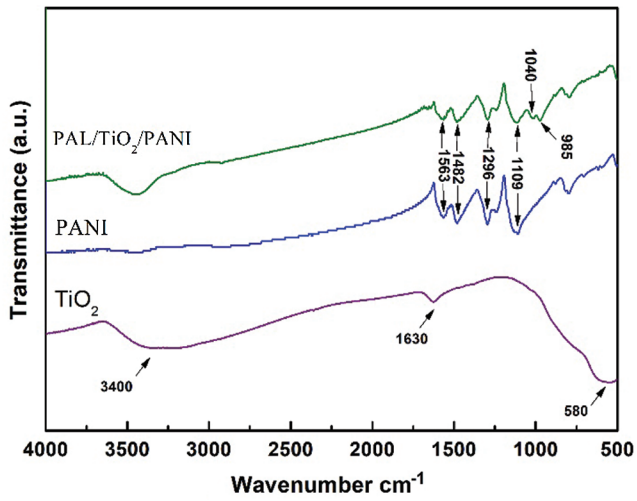

Figure 4: The FT-IR spectra of the TiO_2, PANI and PAL/TiO_2/PANI

3.2 Dielectric Properties

The dielectric properties and polarizability of the particles are the key factors affecting the ER effect. Generally, a good ER effect requires a large dielectric constant difference Δε (Δε = $\varepsilon_{100\ Hz} - \varepsilon_{100\ Hz}$). The dielectric spectra of the TiO_2, PANI and PAL/TiO_2/PANI ER fluids in the frequency range of 50–10^5 Hz are shown in Fig. 5. The results show that the PAL/TiO_2/PANI ER fluid has the highest dielectric constant difference Δε between 10^2 and 10^5 Hz. According to the mechanism of interface polarization [23,24], the larger Δε indicates that the ER fluid can form strong interaction between the particles of ER fluid under the action of external electric field and shear field, and maintain the high degree of chain structure formed by the particles.

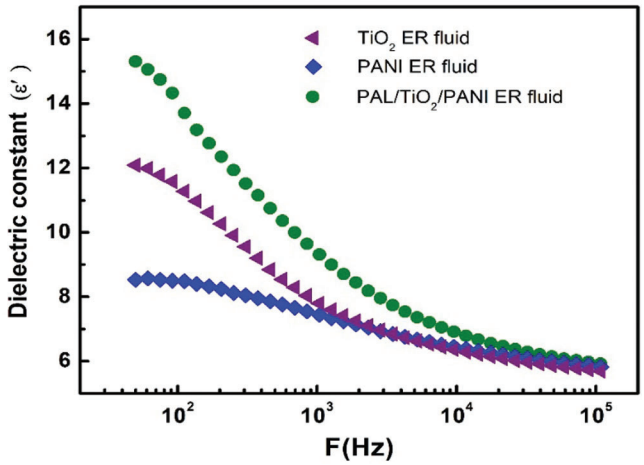

Figure 5: The dielectric spectra of the TiO_2, PANI and PAL/TiO_2/PANI ER fluids

3.3 ER Performance

The yield stresses of the ER fluids containing PAL, TiO_2, PANI, PAL/PANI, PAL/TiO_2 and PAL/TiO_2/PANI nanoparticles under the action of different external electric field are shown in Fig. 6. The corresponding leakage current densities are shown in Fig. 7. The results show that the conventional granular TiO_2 and PANI ER fluids exhibited good ER effect, which is consistent with the previous reports [12,14]. The original PAL ER fluid showed poor ER activity due to its inconspicuous dielectric constant and polarization capacity. As the TiO_2 and PANI nanoparticles were formed on the surface of the PAL rods, the ER activity of the PAL/TiO_2/PANI nanoparticles ER fluid was significantly enhanced. The yield stress of the PAL/TiO_2/PANI nanoparticles ER fluid reached 8.8 kPa under 4 kV mm^{-1} electric field, which was 2.75 times of the TiO_2 ER fluid and 3.38 times of the PANI ER fluid. The enhancement of the ER activity was due to the unique rodlike morphology of the PAL/TiO_2/PANI nanoparticles. Because the charge is concentrated near the end of anisotropic particles, the rod particles are easy to form chain structure along the direction of electric field, and the fiber structure is easier to form between electrodes. In addition, the head-to-head structure of two rod-shaped particles generates an enhanced local electric field, which makes the induced dipole moment and the interaction between particles larger than that of near-spherical particles [25]. Therefore, the one-dimensional suspension of PAL/TiO_2/PANI nanoparticles possesses high yield stress under the action of electric field.

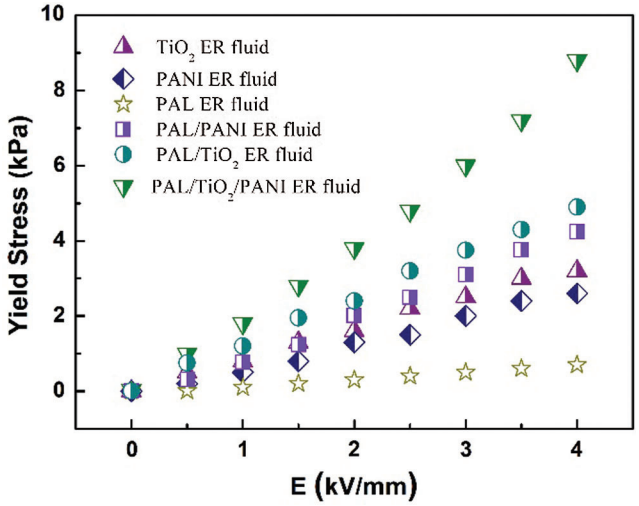

Figure 6: The yield stresses of the ER fluids containing PAL, TiO_2, PANI, PAL/PANI, PAL/TiO_2 and PAL/TiO_2/PANI nanoparticles under the action of different external electric field. The concentration of particles in ER fluid was 15 vol%

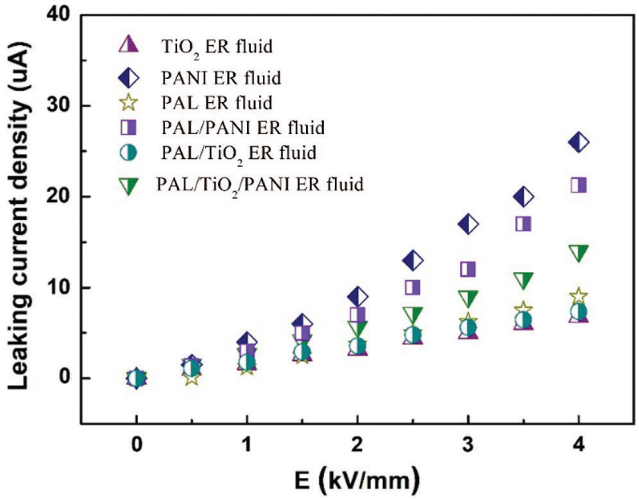

Figure 7: The leaking current density of the PAL, TiO_2, PANI, PAL/PANI, PAL/TiO_2 and PAL/TiO_2/PANI ER fluids under different external electric field. The concentration of particles in ER fluid was 15 vol%

The shear stress of the PAL/TiO_2/PANI ER fluid under different electric fields and shear rates is shown in Fig. 8. Without the external electric field, the PAL/TiO_2/PANI ER fluid shows the traditional Newtonian fluid behavior, the shear stress increases with the increase of shear rate. When the electric field is applied, the PAL/TiO_2/PANI ER fluid exhibits Bingham plastic behavior, which was the typical rheological characteristic of an ER fluid [26,27]. Furthermore, the shear stress as a function of shear rate maintains a stable level in the shear rate range of 0.1–100 s^{-1}. The results show that the PAL/TiO_2/PANI particles not only have high electric polarization force, but also have fast polarization response rate, which makes the particles effectively resist the damage of shear flow to the ER network structure and maintain the stability of the particle network structure in the fluid.

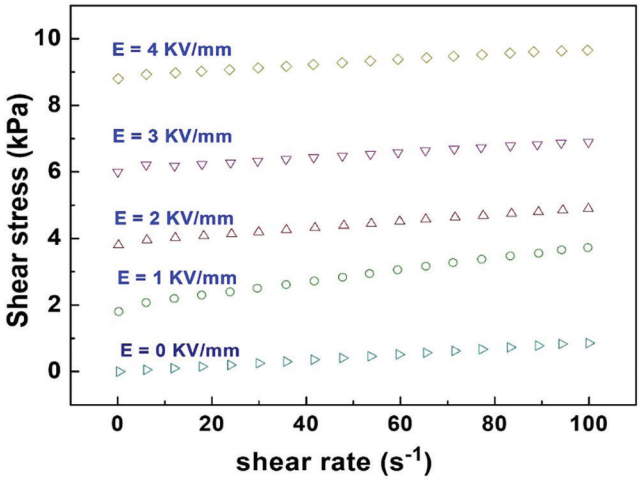

Figure 8: The shear stress of the PAL/TiO_2/PANI ER fluid under different electric fields and shear rates. The concentration of particles in ER fluid was 15 vol%

3.4 Suspension Stability

Suspension stability, especially sedimentation resistance, is one of the important indexes to evaluate whether the material can be widely used, because the ER performance will decrease sharply with the deposition of particles. The suspension stability of ER fluid was characterized by sedimentation ratio test at room temperature. The time-dependent phase separation height between the particle rich phase and the relatively clear oil-rich phase was recorded in a flask. The settling ratio is defined by the percentage of the height of the rich phase relative to the total suspended height. The larger the sedimentation ratio, the better the suspension stability. Fig. 9 shows the sedimentation ratio of ER fluids containing TiO_2, PANI and PAL/TiO_2/PANI at room temperature. After 500 h, the sedimentation rates of TiO_2 and PANI suspensions were 55% and 67%, respectively, while that of rodlike PAL/TiO_2/PANI suspensions was 98%. The enhancement of the suspended stability should be attribute to the distinctive rodlike morphology of PAL/TiO_2/PANI nanoparticles. The large aspect ratio is beneficial to the support between fibrous particles and avoids the large agglomeration of particles. However, it is difficult to establish a supporting role in spherical like particles.

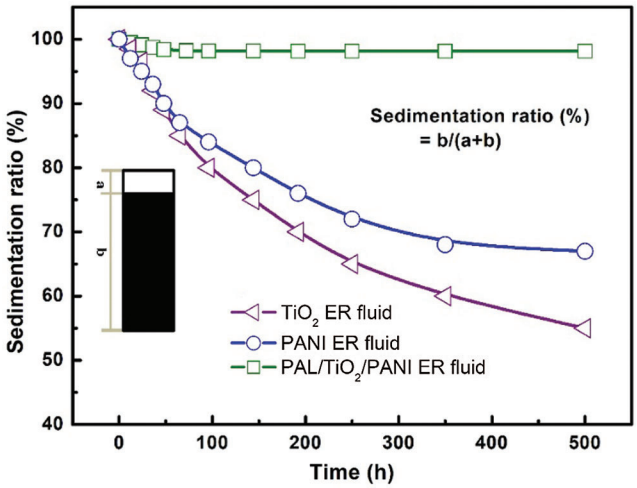

Figure 9: The sedimentation ratios of ER fluids containing TiO_2, PANI and PAL/TiO_2/PANI with time at room temperature

4 Conclusions

The rod-like PAL/TiO_2/PANI nanoparticles was prepared via heterogeneous precipitation and in-situ polymerization process. Compared to conventional TiO_2 or PANI ER fluid, the PAL/TiO_2/PANI ER fluid exhibited distinctly improved polarization capacity and ER activity. The yield stress of the PAL/TiO_2/PANI nanoparticles ER fluid reached 8.8 kPa under 4 kV mm^{-1} electric field, which was 2.75 times of the granular TiO_2 ER fluid and 3.38 times of the granular PANI ER fluid. Furthermore, the shear stress of the PAL/TiO_2/PANI ER fluid could maintain a stable level over the whole shear rate range of 0.1–100 s^{-1}. The PAL/TiO_2/PANI ER fluid also possessed better suspended stability compared to the conventional granular TiO_2 or PANI ER fluid. After standing for 500 h, the sedimentation ratio of the PAL/TiO_2/PANI suspension reached 98%.

Funding Statement: The authors gratefully acknowledge the financial support by the Jiangsu Key R&D program (BE2019072) and the Ningbo Natural Science Foundation (2018A610167 and 2018A610322).

Conflicts of Interest: The authors declare that they have no conflicts of interest to report regarding the present study.

References

1. Halsey, T. C. (1992). Electrorheological fluids. *Science, 258,* 761–766. DOI 10.1126/science.258.5083.761.
2. An, J. S., Moon, I. J., Kwon, S. H., Choi, H. J. (2017). Swelling-diffusion-interfacial polymerized core-shell typed polystyrene/Poly(3, 4-ethylenedioxythiophene) microspheres and their electro-responsive characteristics. *Polymer, 115,* 137–145. DOI 10.1016/j.polymer.2017.03.027.
3. Lee, S., Noh, J., Hong, S., Kim, Y. K., Jang, J. (2016). Dual stimuli-responsive smart fluid of graphene oxide-coated iron oxide/silica core/shell nanoparticles. *Chemistry of Materials, 28,* 2624–2633. DOI 10.1021/acs.chemmater.5b04936.
4. Liu, Y. D., Quan, X., Hwang, B., Kwon, Y. K., Choi, H. J. (2014). Core-Shell-structured monodisperse copolymer/silica particle suspension and its electrorheological response. *Langmuir, 30,* 1729–1734. DOI 10.1021/la4050072.
5. Yoon, C., Lee, G., Noh, J., Lee, C., Cheong, O. J. et al. (2016). A comparative study of the electrorheological properties of various N-doped nanomaterials using ammonia plasma treatment. *Chemical Communications, 52,* 4808–4811. DOI 10.1039/C5CC10201D.
6. Yoon, C., Lee, S., Cheong, O. J., Jang, J. (2015). Enhanced electroresponse of alkaline earth metal doped silica/titania spheres by synergetic effect of dispersion stability and dielectric property. *ACS Applied Materials & Interfaces, 7,* 18977–18984. DOI 10.1021/acsami.5b02388.
7. Wu, J. H., Jin, T., Liu, F. H., Guo, J. J., Cui, P. et al. (2014). Preparation of Rod-like calcium titanyl oxalate with enhanced electrorheological activity and their morphological effect. *Journal of Materials Chemistry A, 2,* 5629–5635. DOI 10.1039/C4TC00691G
8. Lee S., Yoon C., Hong, J. Y., Jang, J. (2014). Enhanced electrorheological performance of a graphene oxide-wrapped silica rod with a high aspect ratio. *Journal of Materials Chemistry C, 2,* 6010–6016. DOI 10.1039/C4TC00635F.
9. Yoon, C. M., Noh, J., Jang, Y., Jang, J. (2017). Fabrication of a silica/titania hollow nanorod and its electroresponsive activity. *RSC Advances, 7,* 19754–19763. DOI 10.1039/C7RA01786C.
10. Sun, W., Song, H., Xi, Z., Ma, J., Wang, B. et al. (2020). Synthesis and enhanced electrorheological properties of TS-1/titanium oxide core/shell nanocomposite. *Industrial & Engineering Chemistry Research, 59,* 1168–1182. DOI 10.1021/acs.iecr.9b05936.
11. Lee, S., Lee, J., Hwang, S. H., Yun, J., Jang, J. (2015). Enhanced electroresponsive performance of double-shell SiO_2/TiO_2 hollow nanoparticles. *ACS Nano, 9,* 4939–4949. DOI 10.1021/nn5068495.

12. Cheng, Y. C., Guo, J. J., Liu, X. H., Sun, A. H., Xu, G. J. et al. (2011). Preparation of uniform titania microspheres with good electrorheological performance and their size effect. *Journal of Materials Chemistry, 21,* 5051–5056. DOI 10.1039/c0jm03378b.
13. Goswami, S., Brehm, T., Filonovich, S., Cidade, M. T. (2014). Electrorheological properties of polyaniline-vanadium oxide nanostructures suspended in silicone oil. *Smart Materials and Structures, 23,* 105012. DOI 10.1088/0964-1726/23/10/105012.
14. Lee, S., Hong, J., Jang, J. (2013). Synthesis and electrical response of polyaniline/poly(styrene sulfonate)-coated silica spheres prepared by seed-coating method. *Journal of Colloid and Interface Science, 398,* 33–38. DOI 10.1016/j.jcis.2013.01.066.
15. Noh, J., Yoon, C. (2016). Enhanced electrorheological activity of polyaniline coated mesoporous silica with high aspect ratio. *Journal of Colloid and Interface Science, 470,* 237–244. DOI 10.1016/j.jcis.2016.02.061.
16. Li, W., Yang, J. P., Wu, Z. X., Wang, J. X., Li, B. et al. (2012). A versatile kinetics-controlled coating method to construct uniform porous TiO_2 shells for multifunctional core-shell structures. *Journal of the American Chemical Society, 134,* 11864–11867. DOI 10.1021/ja3037146.
17. Han, W. J., Choi, H. J. (2019). Synthesis of conducting polymeric nanoparticles in the presence of a polymerizable surfactant and their electrorheological response. *Colloid and Polymer Science, 297,* 781–784. DOI 10.1007/s00396-019-04497-3.
18. Li, Z. H., Liu, F. H., Xu, G. J., Zhang, J. L., Chu, C. Y. (2014). A kinetics-controlled coating method to construct 1D attapulgite/amorphous titanium oxide nanocomposite with high electrorheological activity. *Colloid and Polymer Science, 292,* 3327–3335. DOI 10.1007/s00396-014-3384-8.
19. Xu, J. X., Wang, W. B., Wang, A. Q. (2017). Stable formamide/palygorskite nanostructure hybrid material fortified by high-pressure homogenization. *Powder Technology, 318,* 1–7. DOI 10.1016/j.powtec.2017.05.032.
20. Wang, W. B., Dong, W. K., Tian, G. Y., Sun, L. Y., Wang, Q. et al. (2019). Highly efficient self-template synthesis of porous silica nanorods from natural palygorskite. *Powder Technology, 354,* 1–10. DOI 10.1016/j.powtec.2019.05.075.
21. Lu, Y. S., Dong, W. K., Wang, W. B., Wang, Q., Hui, A. P. et al. (2019). A comparative study of different natural palygorskite clays for fabricating cost-efficient and eco-friendly iron red composite pigments. *Applied Clay Science, 167,* 50–59. DOI 10.1016/j.clay.2018.10.008.
22. Tang, J., Zong, L., Mu, B., Zhu, Y. F., Wang, A. Q. (2018). Preparation and cyclic utilization assessment of palygorskite/carbon composites for sustainable efficient removal of methyl violet. *Applied Clay Science, 161,* 317–325. DOI 10.1016/j.clay.2018.04.039.
23. Hao, T. (2001). Electrorheological fluids. *Advanced Material, 13,* 1847–1857. DOI 10.1002/1521-4095(200112)13:24<1847::AID-ADMA1847>3.0.CO;2-A.
24. Choi, H. J., Jhon, M. S. (2009). Electrorheology of polymers and nanocomposites. *Soft Matter, 5,* 1562–1567. DOI 10.1039/b818368f.
25. Kanu, R. C., Shaw, M. T. (1998). Enhanced electrorheological fluids using anisotropic particles. *Journal of Rheology, 42,* 657–670. DOI 10.1122/1.550944.
26. Yoon, C., Lee, K., Noh, J., Lee, S., Jang, J. (2016). Electrorheological performance of multigramscale mesoporous silica particles with different aspect ratios. *Journal of Materials Chemistry C, 4,* 1713–1719. DOI 10.1039/C5TC04124D.
27. Liu, Y. D., Choi, H. J. (2012). Electrorheological fluids: Smart soft matter and characteristics. *Soft Matter, 8,* 11961–11978. DOI 10.1039/c2sm26179k.